SHP-1 overexpression increases the radioresistance of NPC cells by enhancing DSB repair, increasing S phase arrest and decreasing cell apoptosis

XIAOFEN PAN, JINGJING MOU, SHA LIU, ZIYI SUN, RUI MENG, ZHENWEI ZHOU, GANG WU and GANG PENG

Cancer Center, Union Hospital, Tongji Medical College, Huazhong University of Science and Technology, Wuhan, Hubei 430022, P.R. China

Received February 10, 2015; Accepted March 24, 2015

DOI: 10.3892/or.2015.3939

Abstract. The present study aimed to investigate the influence of SHP-1 on the radioresistance of the nasopharyngeal carcinoma (NPC) cell line CNE-2 and the relevant underlying mechanisms. The human NPC cell line CNE-2 was transfected with a lentivirus that contained the SHP-1 gene or a nonsense sequence (referred to as LP-H1802Lv201 and LP-NegLv201 cells, respectively). Cells were irradiated with different ionizing radiation (IR) doses. Cell survival, DNA double-strand breaks (DSBs), apoptosis, cell cycle distribution, and the expression of related proteins were assessed using colony formation assay, immunofluorescent assays (IFAs), flow cytometry (FCM) and western blot analyses, respectively. Compared with the control (CNE-2 cells) and LP-NegLv201 cells, LP-H1802Lv201 cells were more resistant to IR. IFAs showed that IR caused less histone H2AX phosphorylation (γH2AX) and RAD51 foci in the LP-H1802Lv201 cells. Compared with the control and LP-NegLv201 cells, LP-H1802Lv201 cells showed increased S phase arrest. After IR, the apoptotic rate of the LP-H1802Lv201 cells was lower in contrast to the control and LP-NegLv201 cells. Western blot analyses showed that IR increased the phosphorylation of ataxia telangiectasia mutated (ATM) kinase, checkpoint kinase 2 (CHK2), ataxia telangiectasia and Rad3-related (ATR) protein, checkpoint kinase 1 (CHK1) and p53. In LP-H1802Lv201 cells, the phosphorylation levels of ATM and CHK2 were significantly increased while the p53 phosphorylation level was decreased compared to these levels in the control and LP-NegLv201 cells. Phosphorylation of ATR and CHK1 did not show significant differences in the three cell groups. Overexpression of SHP-1 in the CNE-2 cells led to radioresistance and the radioresistance was related to enhanced DNA DSB repair, increased S phase arrest and decreased cell apoptosis.

Correspondence to: Dr Gang Peng, Cancer Center, Union Hospital, Tongji Medical College, Huazhong University of Science and Technology, 1277 Jiefang Road, Wuhan, Hubei 430022, P.R. China
E-mail: penggang1977@gmail.com

Abbreviations: NPC, nasopharyngeal carcinoma; IR, ionizing radiation; DSB, double-strand break; NSCLC, non-small cell lung cancer; GFP, green fluorescent protein; IFA, immunofluorescent assay; FCM, flow cytometry; DDR, DNA damage repair response; ATM, ataxia telangiectasia mutated; CHK2, checkpoint kinase 2; ATR, ataxia telangiectasia and Rad3-related protein; CHK1, checkpoint kinase 1; NHEJ, non-homologous end joining; TKI, tyrosine kinase inhibitor

Key words: nasopharyngeal carcinoma, tyrosine phosphatase, SHP-1, radioresistance, DNA damage response, cell cycle arrest, apoptosis

Introduction

Nasopharyngeal carcinoma (NPC) is one of the most common cancers in Southern China, Southeast Asia, the Arctic, and the Middle East/North Africa (1). Epstein-Barr virus infection, genetic factors, dietary and environmental factors are risk factors for the development of NPC (2). Due to the unique anatomical location of the nasopharynx where many important nerves and vessels are located, surgery is not the primary choice for NPC treatment. Since NPC cells are sensitive to ionizing radiation (IR), radiotherapy is now the primary therapy for NPC patients (3). However, some carcinoma cells are resistant to IR. These radioresistant cells remain the major cause of local recurrence and metastasis of NPC (4). Therefore, decreasing the radioresistance of NPC cells could help improve NPC patient prognosis.

SHP-1, also called PTPN6 (5), is an SH2 domain-containing protein tyrosine phosphatase (PTP). It consists of 17 exons and 16 introns and spans ~17 kb (6,7). SHP-1 is highly expressed in normal hematopoietic cells (8) and is weakly expressed in several hematological malignancies, including Burkitt's (9), natural killer cell (10) and diffuse large cell lymphomas, Hodgkin's disease (11) and chronic myeloid leukemia (12). However, some studies have found that SHP-1 is highly expressed in certain epithelial carcinoma cells, such as ovarian and breast cell lines (13). Although many studies have been conducted concerning SHP-1 in hematological tumors, the function of SHP-1 in solid tumors, particularly in NPC, is mostly unknown.

Our previous study found that SHP-1 is overexpressed in NPC tissues and is associated with local recurrence after radiotherapy (14). Knockdown of SHP-1 by siRNA in the NPC cell line CNE-2 and in the non-small cell lung cancer (NSCLC) cell line A549 resulted in increased radiosensitivity (15,16). These results suggest that overexpression of SHP-1 may be related to radioresistance.

In the present study, we aimed to further examine whether increased SHP-1 contributes to radioresistance of NPC CNE-2 cells. We also investigated how it is related to DNA double-strand break (DSB) repair, cell cycle arrest and cell apoptosis.

Materials and methods

Cell culture and irradiation procedure. The NPC cell line CNE-2 was obtained from the Cell Bank of the Sun Yat-Sen University (Guangzhou, China) and cultured in RPMI-1640 medium (HyClone, Logan, UT, USA) supplemented with 12% fetal bovine serum (Gibco, Grand Island, NY, USA) and 1% penicillin/streptomycin (HyClone). The cells were maintained at 37˚C in a humidified incubator with 5% CO_2 and 95% room air. Irradiation was performed at room temperature with single doses of X-rays using a linear accelerator (Primus K; Siemens, Munich, Bayern, Germany) with 6-MV photons/100-cm focus-surface distance and a dose rate of 2.0 Gy/min.

SHP-1 is upregulated by lentiviral-mediated gene knock-in. Both the SHP-1 gene sequence and a negative oligo sequence were inserted into pEZ-Lv201-green fluorescent protein (GFP) lentiviral vectors (GeneCopoeia, Guangzhou, China). After confirmation of the constructed plasmids by DNA sequencing, the lentiviruses were then transfected into 293T cells. LP-H1802Lv201 is a lentivirus containing the SHP-1 gene and LP-NegLv201 is a negative control containing a negative oligo sequence. Supernatants containing the lentiviruses were harvested, purified and the titer of lentiviruses was determined. Both lentiviral stocks were transfected into the CNE-2 cells. Fifty microliters of lentivirus stock (LP-H1802Lv201 and LP-NegLv201) was added to the CNE-2 cells. Puromycin (Sigma-Aldrich, St. Louis, MO, USA) was used to screen cells transfected with the lentivirus at a concentration of 2 μg/ml. RNA was extracted and RT-qPCR was used to detect SHP-1 mRNA expression. Total protein was isolated and the expression of SHP-1 was detected by western blotting. The efficiency of infection was observed by fluorescence microscopy.

Colony formation assay. Cells were seeded into 6-well culture plates and irradiated the next day at distinct doses (0, 2, 4, 6 and 8 Gy). The plates were incubated for 14 days, fixed with methanol, and stained with Giemsa (both from Wuhan Google Biotechnology Ltd. Co., Wuhan, China), and colonies containing at least 50 cells were counted as a clone. A multi-target single-hit model was used to describe the survival fraction (SF). The equation $SF = 1-(1 - e^{-D/D0})^N$ (where D is the radiation dose; e is the bottom of the natural logarithm; D_0 is the mean death dose; and N is the extrapolated number) was used to fit the cell survival curves.

Immunofluorescent assay (IFA). Cells were irradiated with 2 Gy of X-rays, and incubated for specified times after IR. The cells were harvested and immunostained with anti-histone H2AX phosphorylation (γH2AX; Abcam, Cambridge, UK) or anti-RAD51 (Millipore, Billerica, MA, USA) antibodies. Then the cells were incubated with Dylight 549 goat-anti-rabbit IgG (Abbkine, Redlands, CA, USA). The nuclei were visualized by staining with Hoechst 33258 (Wuhan Google Biotechnology Ltd. Co.). Images were captured using an Olympus laser scanning confocal microscope (Olympus Optical Co., Tokyo, Honshu, Japan). For each treatment condition, fluorescently labeled γH2AX foci or RAD51 were assessed by fluorescence microscopy in at least 50 cells.

Cell cycle flow cytometry (FCM) analysis. Cells were irradiated with 6 Gy of X-rays and incubated for 24 h after IR. The cells were fixed overnight with 70% ethanol, and resuspended in PBS containing 1 mg/ml RNase and 50 μg/ml propidium iodide (both from Sigma-Aldrich). Cellular DNA content was determined using a FACScan flow cytometer (Becton-Dickinson, San Jose, CA, USA). Quantification of cells in the G1, S, and G2/M phases was performed using CellQuest software (BD Biosciences).

FCM analysis of apoptosis. Cells were exposed to 6 Gy of X-rays and incubated for 24 h after IR. The cells were then collected and resuspended in 200 μl binding buffer and stained with 2 μl Annexin V-APC and 4 μl of 7-AAD (all from Bestbio, Shanghai, China). Analyses were performed using a FACScan flow cytometer (Becton-Dickinson). Both APC- and 7-AAD-positive cells were considered apoptotic cells.

Western blotting. Cells were harvested and lysed after the different treatments. Protein lysate concentrations were determined using the BCA protein assay (Wuhan Google Biotechnology Ltd. Co.). Equal amounts of protein were separated by 8-15% SDS-PAGE (according to molecular weight; Wuhan Google Biotechnology Ltd. Co.) and transferred to PVDF membranes (Millipore). The membranes were blocked with 5% BSA (Wuhan Google Biotechnology Ltd. Co.) and then probed with anti-SHP-1 (Epitomics, Burlingame, CA, USA), anti-RAD51 (Millipore), anti-phospho-p53 (Cell Signaling Technology, Danvers, MA, USA), anti-γH2AX (Abcam), anti-phospho-ATM kinase and anti-phospho-ATR protein (both from Cell Signaling Technology), anti-phospho-CHK1 (Abcam), anti-phospho-CHK2 (Cell Signaling Technology) or anti-GAPDH (Santa Cruz Biotechnology, Inc., Dallas, TX, USA) antibodies. After washing by TBST (Wuhan Google Biotechnology Ltd. Co.), the membranes were incubated with goat-anti-rabbit or goat-anti-mouse IgG (Invitrogen, Carlsbad, CA, USA) and visualized by a chemiluminescence detection system (UVP OptiCam 600; UVP Inc., Upland, CA, USA) using a chemiluminescence kit (Invitrogen). GAPDH protein levels were used as a control to verify equal protein loading. Image J 1.43b software (NIH, Bethesda, MD, USA) was used to scan the protein bands and to measure the optical density values.

RT-qPCR. Total RNA was extracted with TRIzol (Invitrogen), and reverse transcription was used to obtain cDNA, according to the manufacturer's instructions for the Takara RT-PCR kit (Takara, Shiga, Japan). Then, qPCR was performed according

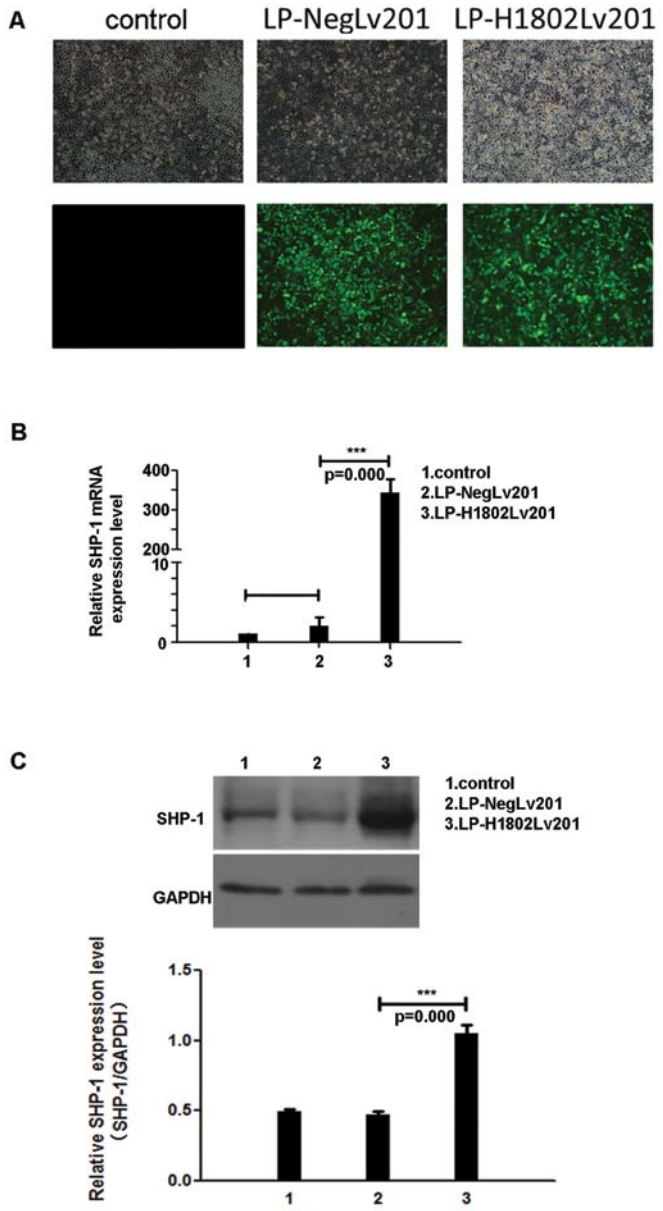

Figure 1. Examination of transfection efficiency. Lentiviral vectors containing the SHP-1 gene (LP-H1802Lv201) or a nonsense sequence (LP-NegLv201) were constructed and transfected into CNE-2 cells. (A) The transfection efficiency was observed by fluorescence microscopy. In the LP-NegLv201 and LP-H1802Lv201 cells, a high level of green fluorescent protein (GFP) was observed, which indicated high transfection efficiency. (B) RT-qPCR was used to determine SHP-1 mRNA expression levels. SHP-1 mRNA showed an ~300-fold increase in the LP-H1802Lv201 cells. (C) Western blot analysis was used to determine SHP-1 expression at the protein level. LP-H1802Lv201 cells showed a significantly increased level of SHP-1. GAPDH served as a loading control. Untreated CNE-2 cells were used as the control. Transfection efficiency was determined by several methods. Data are displayed as mean ± SD from at least three independent experiments; ***p<0.001.

to the manufacturer's instructions using SYBR-Green in a PCR amplifier, ABI Prism 7000 (both from Applied Biosystems, Foster City, CA, USA). The StepOne™ software v2.1 was used to analyze the data. The primer sequences for SHP-1 were: forward, 5'-ACCATCATCCACCTCAAGT ACC-3' and reverse, 5'-CTGAGCACAGAAAGCACGAA-3'. β-actin was used as an internal control, and the primer

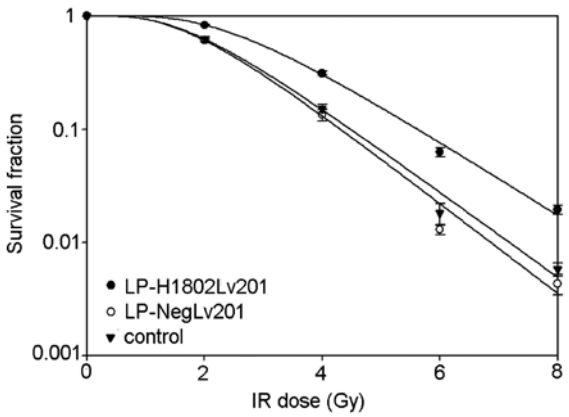

Figure 2. Radiosensitivity is decreased in the SHP-1-overexpressing CNE-2 cells. Colony formation assay was used to examine the radiosensitivity of the cells. Radiosensitivity of the LP-H1802Lv201 cells was obviously decreased, which implied an enhanced radioresistance.

sequences were: forward, 5'-GATGAGATTGGCATGGC TTT-3' and reverse, 5'-CACCTTCACCGTTCCAGTTT-3'.

Statistical analysis. Experimental data are expressed as the mean ± SD from at least three or more independent experiments. Differences in the measured variables of the experimental and control groups were assessed using a t-test (SPSS 21.0 software). The criterion for statistical significance was $p<0.05$.

Results

Overexpression of SHP-1 by lentiviral-mediated gene knock-in in CNE-2 cells. We transfected the NPC cell line CNE-2 with a lentivirus containing the SHP-1 gene or a nonsense sequence (referred to as LP-H1802Lv201 and LP-NegLv201 cells, respectively). Fluorescence microscopy was used to observe GFP intensity and transfection efficiency (Fig. 1A). RT-PCR and western blot analyses were used to detect SHP-1 expression levels at the mRNA and protein levels, respectively. RT-qPCR showed that in the LP-H1802Lv201 cells, SHP-1 mRNA expression levels were increased by 300-fold (Fig. 1B). Western blot analyses also indicated an increased expression of SHP-1 protein in the LP-H1802Lv201 cells (Fig. 1C).

Upregulation of SHP-1 results in enhanced radioresistance. To determine the relationship between SHP-1 and radioresistance, colony formation assays were performed, and cell survival curves were used to analyze the results. The shoulder area under the survival curve was larger in the LP-H1802Lv201 cells (Fig. 2). In contrast to the control and LP-NegLv201 cells, LP-H1802Lv201 cells had increased D_0, D_q, N and SF_2 (Table I) values, which represented a higher radioresistance. The differences in these values were negligible between the control and LP-NegLv201 cells. Therefore, we concluded that upregulation of SHP-1 resulted in enhanced radioresistance.

DNA DSB repair is enhanced in the SHP-1-overexpressing cells. To determine DNA DSB repair, we used an anti-γH2AX to immunofluorescently stain γH2AX foci at different time-points

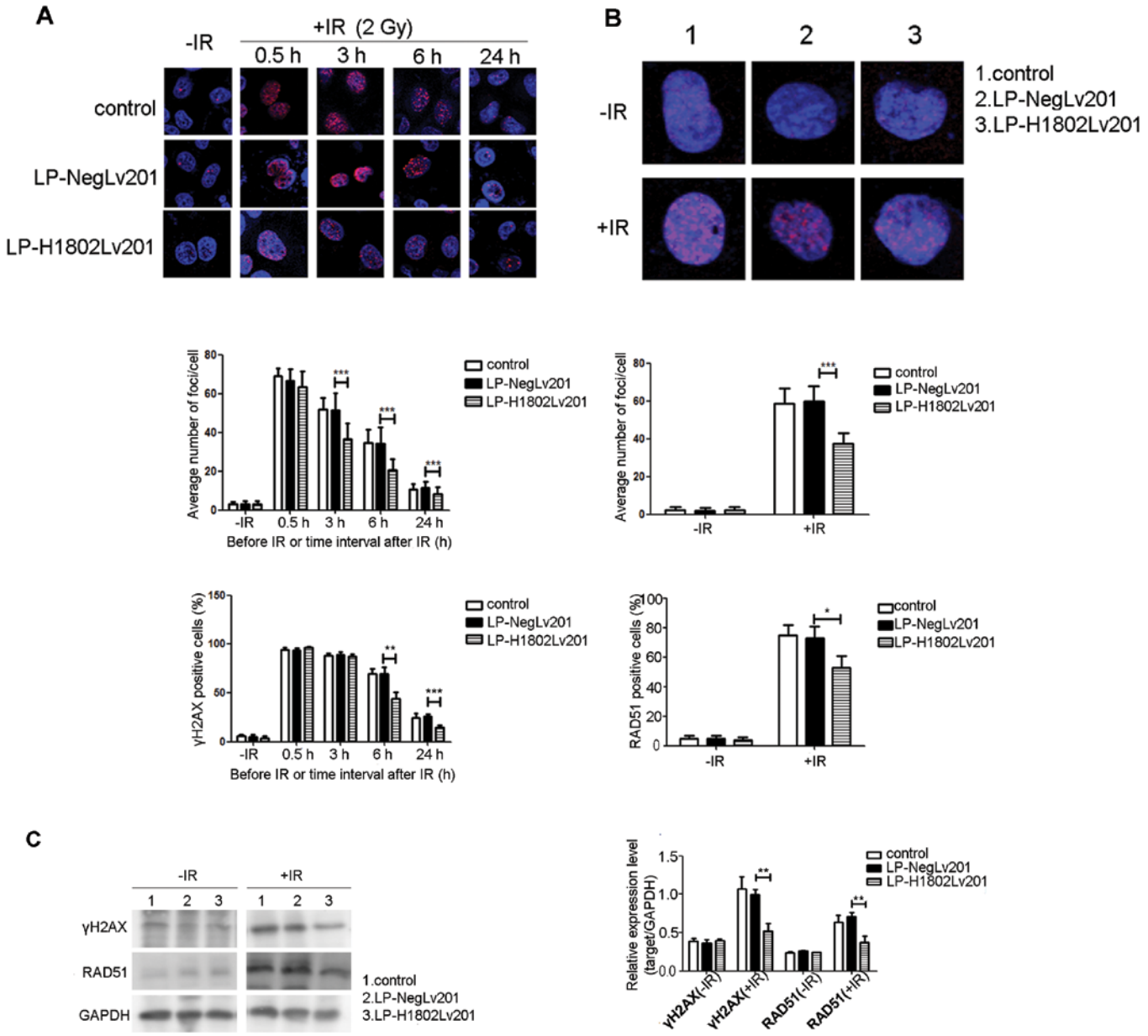

Figure 3. DNA double-strand break (DSB) repair is enhanced in the SHP-1-overexpressing cells. Cells were exposed to 2 Gy of X-rays. (A) Histone H2AX phosphorylation (γH2AX) foci in the 3 cell groups. The average number of γH2AX foci per cell was counted. The percentage of γH2AX-positive cells was also calculated. (B) RAD51 foci in the 3 cell groups. The average number of γH2AX foci per cell was counted. The percentage of RAD51-positive cells was also calculated. (C) Changes in γH2AX and Rad51 protein at 24 h after ionizing radiation (IR). GAPDH was used as a loading control. Following incubation for specific times after IR, cells were immunostained with γH2AX or RAD51 antibodies. Hoechst 33342 was used to visualize nuclei. Data represent the mean ± SD from at least three independent experiments; $^{*}p<0.05$, $^{**}p<0.01$, $^{***}p<0.001$.

Table I. Parameters of the radiosensitivity in the three cell lines.

Parameters	CNE-2	LP-NegLv201	LP-H1802Lv201
D_0	1.153	1.092	1.329
D_q	1.768	1.774	2.255
N	5.078	5.401	7.170
SF_2	0.610	0.627	0.835

D_0, mean lethal dose; D_q, quasi-threshold dose; N, extrapolation number; SF_2, surviving fraction at 2 Gy.

after exposure to IR. As shown in Fig. 3A without exposure to IR, few γH2AX foci were observed in the three cell groups. After irradiation with 2 Gy IR, γH2AX foci rapidly increased. The numbers of γ-H2AX foci in the 3 groups were almost equal at 0.5 h after IR. However, foci in the LP-H1802Lv201 cells disappeared more quickly. In contrast to the control and LP-NegLv201 cells, γH2AX foci in the LP-H1802v201 cells were significantly decreased at 3, 6 and 24 h after IR. Cells having more than 10 γH2AX foci were scored as γH2AX-positive cells. We found that the percentage of γH2AX-positive cells was significantly decreased in the LP-H1802Lv201 cell group at 6 and 24 h after IR. In contrast, at 0.5 and 3 h after

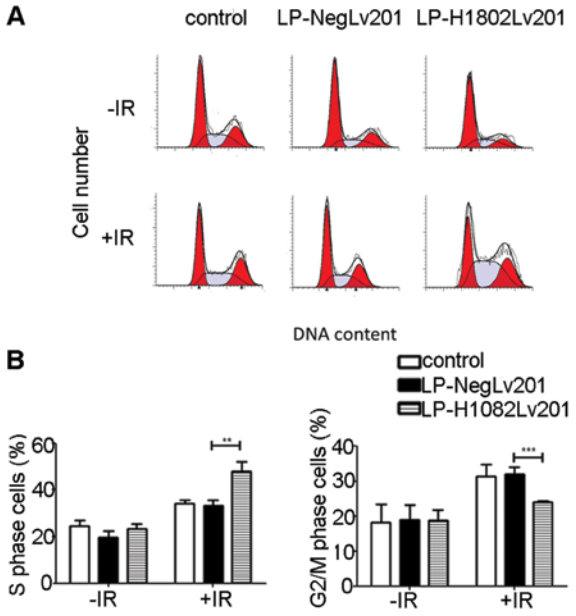

Figure 4. SHP-1 overexpression results in ionizing radiation (IR)-induced S phase arrest. Cells were incubated for 24 h after treatment with IR. (A) Cell cycle distribution was detected by flow cytometry. (B) Histogram of cell cycle distribution. Compared with the control and LP-NegLv201 cells, LP-H1802Lv201 cells showed an increasing S phase arrest and decreased G2/M phase cells after IR. Data represent the mean ± SD from at least three independent experiments; $^{**}p<0.01$, $^{***}p<0.001$.

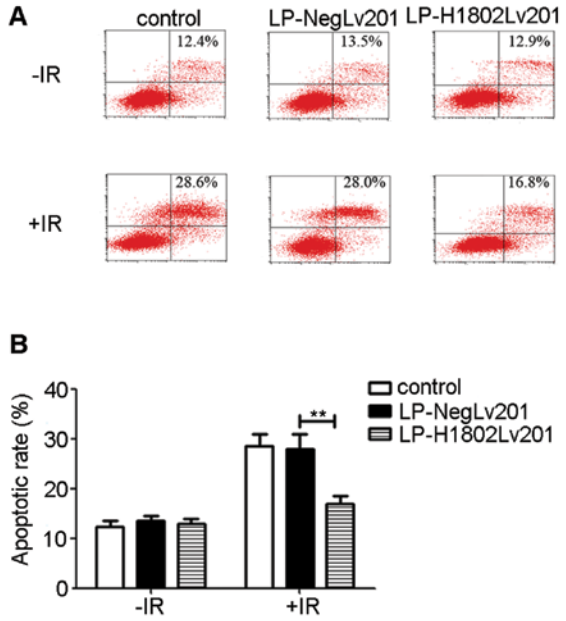

Figure 5. SHP-1 overexpression results in decreased apoptosis. Cells were incutbated for 24 h after treatment with ionizing radiation (IR). (A) Apoptotic rates were determined by flow cytometry. Then apoptosis was determined by flow cytometry. (B) Histogram of apoptotic rates. Compared with the control and LP-NegLv201 cells, the LP-H1802Lv201 cells showed a decrease in cell apoptosis after IR. Data represent the mean ± SD from at least three independent experiments; $^{**}p<0.01$.

IR, the percentages of γH2AX-positive cells in the 3 groups did not differ significantly. We also assessed RAD51 foci at 6 h after IR or under the condition without IR. As shown in Fig. 3B, without IR, RAD51 foci did not show a significant difference in the 3 groups. At 6 h after IR, the number of RAD51 foci in the LP-H1802Lv201 cells was significantly less than that in the control and LP-NegLv201 cells. Cell having more than 10 RAD51 foci were scored as RAD51-positive cells. The percentage of RAD51-positive cells was also lower in the LP-H1802Lv201 cell group. Western blot analyses were also used to assess γH2AX and RAD51 expression at 24 h after IR or under the condition without IR (Fig. 3C). Without IR, expression levels of γH2AX and RAD51 in the 3 cell groups were almost equal. At 24 h after IR, expression levels of γH2AX and RAD51 were significantly increased in contrast to the condition without IR. However, expression levels of γH2AX and RAD51 were lower in the LP-H1802Lv201 cells. We concluded that IR caused DNA DSBs equally in the 3 cell groups. Yet, SHP-1-overexpressing cells showed an enhanced DSB repair capacity.

SHP-1-overexpressing cells undergo increased S phase arrest after IR. To evaluate how SHP-1 affects cell cycle distribution, we used FCM to estimate the cell cycle changes. Without IR, the cell fractions in the S phase did not show a significant difference in the 3 cell groups. At 24 h after IR, the percentage of S phase cells was significantly increased and the percentage of G2/M phase cell group was decreased in the LP-H1802Lv201 cells compared with the control and LP-NegLv201 cells (Fig. 4). The results suggest that overexpression of SHP-1 led to increased IR-induced S phase arrest and thus decreased G2/M phase cells.

Overexpression of SHP-1 causes an anti-apoptotic effect. Before IR, the apoptotic rate of the control, LP-NegLv201 and LP-H1802Lv201 cells had no significant differences. At 24 h after IR, the apoptotic rates of the 3 cell groups were increased. However, the apoptotic rate of the LP-H1802Lv201 cells was significantly lower than the rate in the control and LP-NegLv201 cells (Fig. 5). These data suggest that IR promoted apoptosis in the 3 cell groups. However, LP-H1802Lv201 cells were more resistant to IR-induced apoptosis. The results suggest that overexpression of SHP-1 had an anti-apoptotic effect.

SHP-1-overexpressing cells show increased activation of ATM and CHK2 and suppressed activation of p53 after IR. To explore how the ATM/CHK1 and ATR/CHK1 pathways were activated after IR, we determined the phosphorylation levels of ATM (p-ATM), CHK2 (p-CHK2), ATR (p-ATR), CHK1 (p-CHK1) and p53 (p-p53). Results of the western blot analyses showed that the phosphorylation levels of ATM, CHK2, ATR, CHK1 and p53 were extremely low when cells did not receive IR. After radiation, phosphorylation levels of these proteins were increased. Compared with the control and LP-Neglv201 cells, LP-H1802lv201 cells had relatively increased phosphorylation levels of ATM and CHK2, while the phosphorylation of p53 was decreased. Phosphorylation of ATR and CHK1 did not show a significantly difference (Fig. 6).

Discussion

In the past few decades, SHP-1 has been believed to be a tumor-suppressor in many malignancies (10,17,18). However, our previous research found that SHP-1 was overexpressed in NPC tissues and was associated with local recurrence

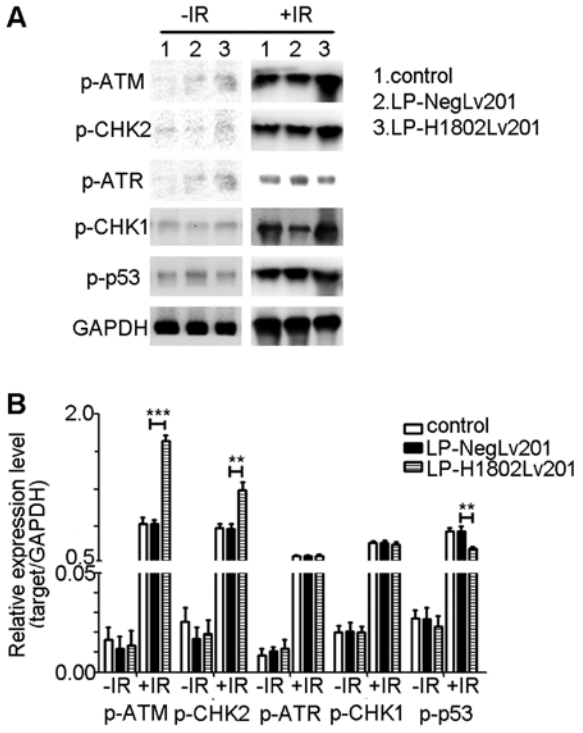

Figure 6. Effects of SHP-1 on IR-induced activation of the ATM/CHK2 and ATR/CHK1 pathways and p53. (A) Western blot results. Effects of SHP-1 overexpression on IR-induced phosphorylation of ATM/CHK2 and ATR/CHK1 pathways and p53 at 24 h after IR. (B) Optical density values. GAPDH was used as a loading control. Data represent the mean ± SD from at least three independent experiments; $^{**}p<0.01$, $^{***}p<0.001$. IR, ionizing radiation; ATM, ataxia telangiectasia mutated kinase; CHK2, checkpoint kinase 2; ATR, ataxia telangiectasia and Rad3-related protein.

and metastasis after radiotherapy (4). Suppression of SHP-1 expression resulted in a higher radiosensitivity (15,16). These results suggest that overexpression of SHP-1 may be related to radioresistance and that it may be a potential target to enhance NPC radiosensitivity.

In the present study, we investigated the effects of SHP-1 on the radioresistance of NPC cells. We showed that overexpression of SHP-1 enhanced DNA DSB repair, increased IR-induced S phase arrest and decreased cell apoptosis, thus resulting in radioresistance in CNE-2 cells. The result was consistent with previous observations (15,16).

IR-induced cell death is a result of irreparable DSBs (19). The repair response of DSBs is one of the factors that influences radiosensitivity. DSBs are mainly repaired by non-homologous end joining (NHEJ) and homologous recombination. Repair of DSBs appeared within 30-60 min after radiation. The majority of DSBs are repaired in 24 h. γH2AX is a hallmark of DSB recognition and repair. Fewer γH2AX foci represent a more rapid repair of DSBs and higher radioresistance (19-24). RAD51 is an important protein involved in homologous recombination processes. Increased RAD51 expression is related to radioresistance of tumor cells (25). In the present study, we showed that overexpression of SHP-1 in NPC cells decreased the expression of γH2AX, which indicted enhanced repair of DSBs. Notably, RAD51 expression was decreased in the LP-H1802lv201 cells, which are relatively radioresistant cells. One reason for this result may be that we detected RAD51 expression only at one time-point after IR. According to γH2AX expression, LP-H1802Lv201 cells had an enhanced DSB repair capacity. Thus, the DSB repair peak of LP-H1802Lv201 cells should have appeared sooner than the control and LP-NegLv201 cells. When we detected the expression of RAD51, the DSB repair peak may have transpired in the LP-H1802lv201 cells while this peak was not yet achieved in the control and LP-Neglv201 cells.

Cells often respond to IR-induced DSBs by activating cell cycle checkpoints, which play an importance role in determining radiosensitivity. In general, S phase cells are the most radioresistant, while G2/M phase cells are the most sensitive to radiation (26). It has been reported that abrogation of the G2/M checkpoint promotes IR-induced cell death (27). The present data showed that overexpression of SHP-1 increased the fraction of S phase cells. At the same time, the cell fraction in the G2/M phase was decreased, which may have resulted from S phase arrest. Thus, we inferred that overexpression of SHP-1 contributed to the radioresistance of NPC cells by increasing S phase arrest.

ATM kinase plays vital roles in IR-induced DNA damage repair response (DDR). ATM is activated upon DNA damage, and downstream effector kinases of ATM, including CHK2 and p53, are also activated (28). Increased activation of ATM/CHK2 enhances DNA damage repair, thus leading to radioresistance. It has been reported that inhibition of ATM activation increases apoptosis and enhances radiosensitivity. The ATR/CHK1 pathway also has an influence on radioresistance by regulating homologous recombination repair. Overactivation of the ATR/CHK1 pathway increased the radioresistance of tumor cells. When DNA damage is not repaired, cells will be eliminated though different mechanisms including p53-dependent apoptosis (28-32). In the present study, we found that SHP-1-overexpressing cells had an increased phosphorylation of the ATM/CHK2 pathway, while phosphorylation of the ATR/CHK1 pathway did not show a difference in the other two cell groups. These data suggest that overexpression of SHP-1 enhanced DNA damage repair by activating the ATM/CHK1 pathway, but not the ATR/CHK1 pathway, and enhanced DNA damage repair resulted in decreased p53-dependent apoptosis.

ATM also takes part in intra-S checkpoint response to IR-induced DSBs through two separate pathways (33,34). One pathway involves activation of CHK1, CHK2 and Cdc25A. CHK1 and CHK2 are phosphorylated and activated by ATM, which leads to phosphorylation and proteolysis of Cdc25A and then activates intra-S checkpoint response (35). The other pathway involves the cohesin subunits, Smc1 and Smc3. Smc1 and Smc3 are phosphorylated by ATM and bind to Scc1 and SA1 or SA2 to form cohesin, which plays important roles in homologous recombination repair of DSBs (33,34,36-38). In the present study, SHP-1-overexpressing cells showed an increased S phase arrest accompanied by increased ATM and CHK2 activation after IR. However, activation of CHK1 was not increased in the SHP-1-overexpressing cells. We inferred that IR-induced DSBs activated the ATM/CHK2 pathway. Then Cdc25A was phosphorylated and the intra-S checkpoint was activated, leading to S phase arrest. However, whether the ATR/CHK1 pathway and ATM/Smc1/Smc3 are involved in S phase arrest in SHP-1-overexpressing cells needs further study.

In the present study, we demonstrated that overexpression of SHP-1 was related to the acquired resistance to IR in the NPC cell line CNE-2. Enhanced DSB repair, increased S phase arrest and decreased apoptosis contributed to this acquired radioresistance. Examining the SHP-1 expression level in tumor tissues of NPC patients may help to predict prognosis.

Acknowledgements

The present study was supported by grants from the Natural Sciences Foundation of China (no. 81301976) and the Wu Jieping Medical Foundation.

References

1. Chang ET and Adami HO: The enigmatic epidemiology of nasopharyngeal carcinoma. Cancer Epidemiol Biomarkers Prev 15: 1765-1777, 2006.
2. Hung CM, Chang CC, Lin CW, Chen CC and Hsu YC: GADD45γ induces G2/M arrest in human pharynx and nasopharyngeal carcinoma cells by cucurbitacin E. Sci Rep 4: 6454, 2014.
3. Lee AW, Sze WM, Au JS, Leung SF, Leung TW, Chua DT, Zee BC, Law SC, Teo PM, Tung SY, *et al*: Treatment results for nasopharyngeal carcinoma in the modern era: the Hong Kong experience. Int J Radiat Oncol Biol Phys 61: 1107-1116, 2005.
4. Feng XP, Yi H, Li MY, Li XH, Yi B, Zhang PF, Li C, Peng F, Tang CE, Li JL, *et al*: Identification of biomarkers for predicting nasopharyngeal carcinoma response to radiotherapy by proteomics. Cancer Res 70: 3450-3462, 2010.
5. Lorenz U: SHP-1 and SHP-2 in T cells: two phosphatases functioning at many levels. Immunol Rev 228: 342-359, 2009.
6. Banville D, Stocco R and Shen SH: Human protein tyrosine phosphatase 1C (PTPN6) gene structure: alternate promoter usage and exon skipping generate multiple transcripts. Genomics 27: 165-173, 1995.
7. Evren S, Wan S, Ma XZ, Fahim S, Mody N, Sakac D, Jin T and Branch DR: Characterization of SHP-1 protein tyrosine phosphatase transcripts, protein isoforms and phosphatase activity in epithelial cancer cells. Genomics 102: 491-499, 2013.
8. Nakase K, Cheng J, Zhu Q and Marasco WA: Mechanisms of SHP-1 P2 promoter regulation in hematopoietic cells and its silencing in HTLV-1-transformed T cells. J Leukoc Biol 85: 165-174, 2009.
9. Delibrias CC, Floettmann JE, Rowe M and Fearon DT: Downregulated expression of SHP-1 in Burkitt lymphomas and germinal center B lymphocytes. J Exp Med 186: 1575-1583, 1997.
10. Oka T, Yoshino T, Hayashi K, Ohara N, Nakanishi T, Yamaai Y, Hiraki A, Sogawa CA, Kondo E, Teramoto N, *et al*: Reduction of hematopoietic cell-specific tyrosine phosphatase SHP-1 gene expression in natural killer cell lymphoma and various types of lymphomas/leukemias: combination analysis with cDNA expression array and tissue microarray. Am J Pathol 159: 1495-1505, 2001.
11. Sato K, Horiuchi M, Yo R and Nakarai I: A long survival case of small cell lung cancer synchronized with renal cancer. Kyobu Geka 44: 251-253, 1991 (In Japanese).
12. Amin HM, Hoshino K, Yang H, Lin Q, Lai R and Garcia-Manero G: Decreased expression level of SH2 domain-containing protein tyrosine phosphatase-1 (Shp1) is associated with progression of chronic myeloid leukaemia. J Pathol 212: 402-410, 2007.
13. López-Ruiz P, Rodriguez-Ubreva J, Cariaga AE, Cortes MA and Colás B: SHP-1 in cell-cycle regulation. Anticancer Agents Med Chem 11: 89-98, 2011.
14. Duró JC: Postmenopausal osteoporosis. Med Clin (Barc) 85: 506-509, 1985 (In Spanish).
15. Peng G, Cao RB, Li YH, Zou ZW, Huang J and Ding Q: Alterations of cell cycle control proteins SHP 1/2, p16, CDK4 and cyclin D1 in radioresistant nasopharyngeal carcinoma cells. Mol Med Rep 10: 1709-1716, 2014.
16. Cao R, Ding Q, Li P, Xue J, Zou Z, Huang J and Peng G: SHP1-mediated cell cycle redistribution inhibits radiosensitivity of non-small cell lung cancer. Radiat Oncol 8: 178, 2013.
17. Schibli RA: Lung biopsy in interstitial pulmonary processes. Schweiz Med Wochenschr 106: 467-468, 1976 (In German).
18. Tassidis H, Culig Z, Wingren AG and Härkönen P: Role of the protein tyrosine phosphatase SHP-1 in interleukin-6 regulation of prostate cancer cells. Prostate 70: 1491-1500, 2010.
19. Jackson SP and Bartek J: The DNA-damage response in human biology and disease. Nature 461: 1071-1078, 2009.
20. Reynolds P, Anderson JA, Harper JV, Hill MA, Botchway SW, Parker AW and O'Neill P: The dynamics of Ku70/80 and DNA-PKcs at DSBs induced by ionizing radiation is dependent on the complexity of damage. Nucleic Acids Res 40: 10821-10831, 2012.
21. Jakob B, Splinter J, Conrad S, Voss KO, Zink D, Durante M, Löbrich M and Taucher-Scholz G: DNA double-strand breaks in heterochromatin elicit fast repair protein recruitment, histone H2AX phosphorylation and relocation to euchromatin. Nucleic Acids Res 39: 6489-6499, 2011.
22. Lieber MR: The mechanism of double-strand DNA break repair by the nonhomologous DNA end-joining pathway. Annu Rev Biochem 79: 181-211, 2010.
23. Schmid TE, Dollinger G, Beisker W, Hable V, Greubel C, Auer S, Mittag A, Tarnok A, Friedl AA, Molls M, *et al*: Differences in the kinetics of gamma-H2AX fluorescence decay after exposure to low and high LET radiation. Int J Radiat Biol 86: 682-691, 2010.
24. Rao VA, Agama K, Holbeck S and Pommier Y: Batracylin (NSC 320846), a dual inhibitor of DNA topoisomerases I and II induces histone gamma-H2AX as a biomarker of DNA damage. Cancer Res 67: 9971-9979, 2007.
25. Maacke H, Jost K, Opitz S, Miska S, Yuan Y, Hasselbach L, Lüttges J, Kalthoff H and Stürzbecher HW: DNA repair and recombination factor Rad51 is over-expressed in human pancreatic adenocarcinoma. Oncogene 19: 2791-2795, 2000.
26. Hall EJ and Giaccia A (eds): Cell survival curves. In: Radiobiology for the Radiologist. 7th edition, Lippincott Williams and Wilkins, New York, NY, 2011.
27. Feng Z, Xu S, Liu M, Zeng YX and Kang T: Chk1 inhibitor Gö6976 enhances the sensitivity of nasopharyngeal carcinoma cells to radiotherapy and chemotherapy in vitro and in vivo. Cancer Lett 297: 190-197, 2010.
28. Zhou W, Sun M, Li GH, Wu YZ, Wang Y, Jin F, Zhang YY, Yang L and Wang DL: Activation of the phosphorylation of ATM contributes to radioresistance of glioma stem cells. Oncol Rep 30: 1793-1801, 2013.
29. Biddlestone-Thorpe L, Sajjad M, Rosenberg E, Beckta JM, Valerie NC, Tokarz M, Adams BR, Wagner AF, Khalil A, Gilfor D, *et al*: ATM kinase inhibition preferentially sensitizes p53-mutant glioma to ionizing radiation. Clin Cancer Res 19: 3189-3200, 2013.
30. Hu B, Wang H, Wang X, Lu HR, Huang C, Powell SN, Huebner K and Wang Y: Fhit and CHK1 have opposing effects on homologous recombination repair. Cancer Res 65: 8613-8616, 2005.
31. Wang H, Wang H, Powell SN, Iliakis G and Wang Y: ATR affecting cell radiosensitivity is dependent on homologous recombination repair but independent of nonhomologous end joining. Cancer Res 64: 7139-7143, 2004.
32. Wang H, Hu B, Liu R and Wang Y: CHK1 affecting cell radiosensitivity is independent of non-homologous end joining. Cell Cycle 4: 300-303, 2005.
33. Yazdi PT, Wang Y, Zhao S, Patel N, Lee EY and Qin J: SMC1 is a downstream effector in the ATM/NBS1 branch of the human S-phase checkpoint. Genes Dev 16: 571-582, 2002.
34. Falck J, Petrini JH, Williams BR, Lukas J and Bartek J: The DNA damage-dependent intra-S phase checkpoint is regulated by parallel pathways. Nat Genet 30: 290-294, 2002.
35. Kaufmann WK: The human intra-S checkpoint response to UVC-induced DNA damage. Carcinogenesis 31: 751-765, 2010.
36. Kim ST, Xu B and Kastan MB: Involvement of the cohesin protein, Smc1, in Atm-dependent and independent responses to DNA damage. Genes Dev 16: 560-570, 2002.
37. Luo H, Li Y, Mu JJ, Zhang J, Tonaka T, Hamamori Y, Jung SY, Wang Y and Qin J: Regulation of intra-S phase checkpoint by ionizing radiation (IR)-dependent and IR-independent phosphorylation of SMC3. J Biol Chem 283: 19176-19183, 2008.
38. Sørensen CS, Syljuåsen RG, Falck J, Schroeder T, Rönnstrand L, Khanna KK, Zhou BB, Bartek J and Lukas J: Chk1 regulates the S phase checkpoint by coupling the physiological turnover and ionizing radiation-induced accelerated proteolysis of Cdc25A. Cancer Cell 3: 247-258, 2003.